Aerospace Science and Technology 32 (2014) 103–110

Contents lists available at ScienceDirect

Aerospace Science and Technology

www.elsevier.com/locate/aescte

# An airfoil shape optimization technique coupling PARSEC parameterization and evolutionary algorithm

Pierluigi Della Vecchia [a,*], Elia Daniele [b], Egidio D'Amato [c]

[a] University of Naples "Federico II", Via Claudio 21, 80125 Naples, Italy
[b] Fraunhofer IWES, Ammerländer Heerstr. 136, 26129 Oldenburg, Germany
[c] Second University of Naples, Via Roma 29, 81031 Aversa (CE), Italy

ARTICLE INFO

*Article history:*
Received 29 May 2013
Received in revised form 22 November 2013
Accepted 22 November 2013
Available online 27 November 2013

*Keywords:*
PARSEC
Genetic algorithm
Games Theory
Nash equilibrium

ABSTRACT

In this work an innovative optimization process for airfoil geometry design is introduced. This procedure is based on the coupling of a PARSEC parameterization for airfoil shape and a genetic algorithms (GA) optimization method to find Nash equilibria (NE). While the PARSEC airfoil parameterization method has the capability to faithfully describe an airfoil geometry using typical engineering parameters, on the other hand the Nash game theoretical approach allows each player to decide, with a more physical correspondence between geometric parameters and objective function, in which direction the airfoil shape should be modified. As a matter of fact the optimization under NE solutions would be more attractive to use when a well posed distinction between players variables exists.

© 2013 Elsevier Masson SAS. All rights reserved.

## 0. Introduction

Airfoil shape optimization is today a common practice used in aerospace and mechanical engineering field. As outlined in Song and Keane [27], the airfoil aerodynamic design can be divided into two main approaches: Inverse Design (ID) and Direct Numerical Optimization (DNO). The first method relates to search an airfoil shape able to satisfy a fluid dynamic characteristic (such as the pressure or the skin friction distribution). On the other hand, DNO methods couple a geometry definition and aerodynamic analysis code in an iterative process to produce optimum design subject to various constraints. However both the approaches share the need to modify airfoil geometry to achieve the goal. Depending on whether the goal is achieved through a small local airfoil modification or a completely new design, different methods of shape parameterization must be employed. Local airfoil shape modifications are usually obtained by smooth perturbations of the original airfoil coordinates through analytical function, such as Legendre, Chebyschev or Bernstein polynomials [14,22,15]. These methods have the advantage of smooth local modifications, although they have no direct relation to geometry and this could lead to undulating curves [15]. The design of a new concept airfoil needs a parameterization method able to accommodate a wider range of new shapes. In the literature several airfoil shape parameterizations can be found. A survey on parameterization method can be seen in Samareh [23]. B-splines and Bezier curves have been widely used to fit airfoil shapes via interpolation methods [8,11]. These methods are very useful to reconstruct and optimize an airfoil (using several artifices on geometry curvatures) but they give some problems due to the difficulties to manage the control points' relative position. Analytical functions have also been derived to represent families of airfoils, as reported in the work of Hicks and Henne [13]. Although this method results very powerful to represent several families of airfoil, it cannot be useful in a radical new concept design. More physically intuitive method enables the use typical airfoil parameters to define the airfoil shape such as leading edge radius, airfoil thickness or trailing edge angle. A methodology of this type is presented by Sobieczky [25,26] and it is called PARSEC. This method uses 11 parameters to represent an airfoil. These parameters are directly linked to the airfoil geometry (thickness, curvature, maximum thickness abscissa, etc.) and they give to a designer the real concept of what will be the design. The geometry definition must be subsequently coupled with an optimization technique which must properly takes into account of the airfoil parameterization. In this work an innovative optimization process for airfoil geometry is introduced. This procedure is based on the coupling of a PARSEC parameterization for geometries and a genetic algorithms (GA) optimization method to find a Nash equilibrium solution. Then the results are compared with the classical Pareto front ones. Many of the past and current optimization processes extensively adopt PARSEC parameterization [25,26] procedure within evolutionary or gradient-based optimization to find the Pareto's front [15,16,20], while Bezier or Hicks–Henne parameterizations are employed with evolutionary or gradient-based

* Corresponding author.
*E-mail addresses:* pierluigi.dellavecchia@unina.it (P. Della Vecchia), elia.daniele@iwes.fraunhofer.de (E. Daniele), egidio.damato@unina2.it (E. D'Amato).

1270-9638/$ – see front matter © 2013 Elsevier Masson SAS. All rights reserved.
http://dx.doi.org/10.1016/j.ast.2013.11.006

**Nomenclature**

| | | | |
|---|---|---|---|
| $\alpha$ | angle of attack | $E$ | aerodynamic efficiency |
| $C_d$ | drag coefficient | $M_\infty$ | Mach number |
| $C_l$ | lift coefficient | $\mathrm{Re}_\infty$ | Reynolds number |
| $C_P$ | pressure coefficient | $\tau$ | airfoil thickness |

algorithm to find Nash equilibrium (NE) [21,29,30]. Of course there are present also proposals concerning hybrid geometry reconstruction methodology [8] as well as surveys on different shape reconstruction methods [3,24,31]. The main valuable contribution of this work is to join the PARSEC parameterization method with NE solution. From an engineering point of view PARSEC has the intrinsic capability of relate airfoil definition in terms of design variables to aerodynamic coefficient behavior, since it would be intuitive linking leading edge radius or maximum thickness abscissa with drag coefficient or camber and trailing edge angle with stall lift coefficient or pitch moment coefficient. On the other hand, the optimization under NE solutions would be more attractive to use when a well posed distinction between players variables exists. Here the PARSEC design variables are intended to play the role of game players' variables. The optimization procedure that couple GA with Games Theory equilibrium solutions has been implemented in a numerical code which has been validated in several test cases among different application fields (engineering CAE [28], location–allocation problem [18], coalition for International Environmental Agreements [17]). In Section 1 the evolutionary optimization algorithm that finds the Nash equilibrium is described, while in Section 2 the coupling procedure between the optimization algorithm and the parameterization method is discussed. In Section 3 the results are shown and the conclusions are summarized in Section 4.

## 1. The Nash GA

In the Nash equilibrium solution concept no player has anything to gain by changing only his own strategy unilaterally [2]. Reducing the general formulation to a two-player situation, the mathematical expression for the Nash equilibrium problem $N$ is:

$$\begin{cases} \text{find}(\bar{x}_1, \bar{x}_2) \in X_1 \times X_2 \quad \text{such that} \\ f_1(\bar{x}_1, \bar{x}_2) = \min\limits_{x_1 \in X_1} f_1(x_1, \bar{x}_2) \\ f_2(\bar{x}_1, \bar{x}_2) = \min\limits_{x_2 \in X_2} f_2(\bar{x}_1, x_2) \end{cases} \tag{1}$$

where $(x_1, x_2) \in X_1 \times X_2$ are the players' variables or strategies, defined in their own strategy domain, while $f_1, f_2$ are the players' objective functions. In particular, for the proposed methodology the players' variables would be in their selves a variables' set, as $x_1 = [\xi_1, \ldots, \xi_n]$, $x_2 = [\eta_1, \ldots, \eta_m]$ of dimension $n, m$ depending on the variables partitioning case introduced by the airfoil geometry reconstruction method (see Section 2). The GA is an adaptive heuristic search method based on the principles of genetics and natural selection. In analogy to living organisms in nature, a GA allows the evolution of a population under specified selection rules so that they aim to a state that maximizes the fitness (i.e. usually minimizes the cost function). A genetic algorithm consists of: (i) a finite population of individuals of assigned size, each of them usually encoded as a string of bits named genotype; (ii) an adaptive function, called fitness, which provides a measure of the individual to adapt to the environment, that is an estimate of the goodness of the solution and an indication on the individuals most likely to reproduce; (iii) semi random genetic operators such as selection, crossover and mutation that operate on the genotype expression of individuals, changing their associated fitness. Constraints can be implemented using penalty functions, which penalize the individual, decreasing the related fitness. The large population that gives the GA more power in solution is also its bane in simple problems [12]. In respect with traditional methods, GA needs more computational time due to the time spent in the objective function calls, but it has got several advantages:

- use of continuous or discrete variables;
- trend of the objective function and its derivatives can be unknown;
- deal with problems with a large number of variables;
- naturally inspired parallelization of the algorithm;
- good results also in problems with extremely complex cost surfaces (with a lot of local minimum);
- proper working with numerically generated and/or experimental data.

Thanks to these advantages the GA produces good results when traditional optimization approaches fail. In the following it is presented the algorithm for a two-player Nash equilibrium game [5,4]. Let $U, V$ be players' strategy sets. Let $f_1$, $f_2$ be two real valued functions defined on $U \times V$ representing the players' cost functions. The algorithm is based on the Nash adjustment process [10], where players take turns setting their outputs, and each player's chosen output is a best response to the output his opponent chosen the period before. If the process does converge, the steady state is a Nash equilibrium of the game. Let $s = u, v$ be the string (or individual, or chromosome) representing the potential solution for a 2 person Nash problem. Then $u$ denotes the subset of variables handled by player 1, belonging to a metric space $U$, and optimized under an objective function always denoted by $f_1$. Similarly $v$ indicates the subset of variables handled by player 2, belonging to metric space $V$, and optimized along another objective function denoted by $f_2$. Thus, as advocated by Nash equilibrium definition [19], player 1 optimizes the chromosome with respect to the first objective function by modifying $u$ while $v$ is fixed by player 2; symmetrically, player 2 optimizes the chromosome with respect to the second criterion by modifying $v$, while $u$ is fixed by player 1. Let $u^{k-1}$ and $v^{k-1}$ be the best values found by players 1 and 2, respectively, at generation $k-1$. At generation $k$, player 1 optimizes $u^k$ using $v^{k-1}$ in order to evaluate the chromosome (now $\mathbf{s} = u^k, v^{k-1}$). At the same time player 2 optimizes $v^k$ using $u^{k-1}$ to evaluate his chromosome (in this case $\mathbf{s} = u^{k-1}, v^k$). The algorithm is organized in several steps that consist of (see Fig. 1):

1. Creating two different random populations, one for each player only at the first generation. Player 1's optimization task is performed by population 1 and *vice versa*.
2. The classification is made on the basis of the evaluation of a fitness function, typical of GAs, that takes into account the results of matches between each individual of population 1 with all individuals of population 2, scoring 1 or $-1$, respectively, for a win or loss, and 0 for a draw.

$$\begin{cases} \text{if } f_1\left(u_i^k, v^{k-1}\right) > f_1\left(u^{k-1}, v_i^k\right), & \text{fitness}_1 = 1 \\ \text{if } f_1\left(u_i^k, v^{k-1}\right) < f_1\left(u^{k-1}, v_i^k\right), & \text{fitness}_1 = -1 \\ \text{if } f_1\left(u_i^k, v^{k-1}\right) = f_1\left(u^{k-1}, v_i^k\right), & \text{fitness}_1 = 0 \end{cases} \tag{2}$$

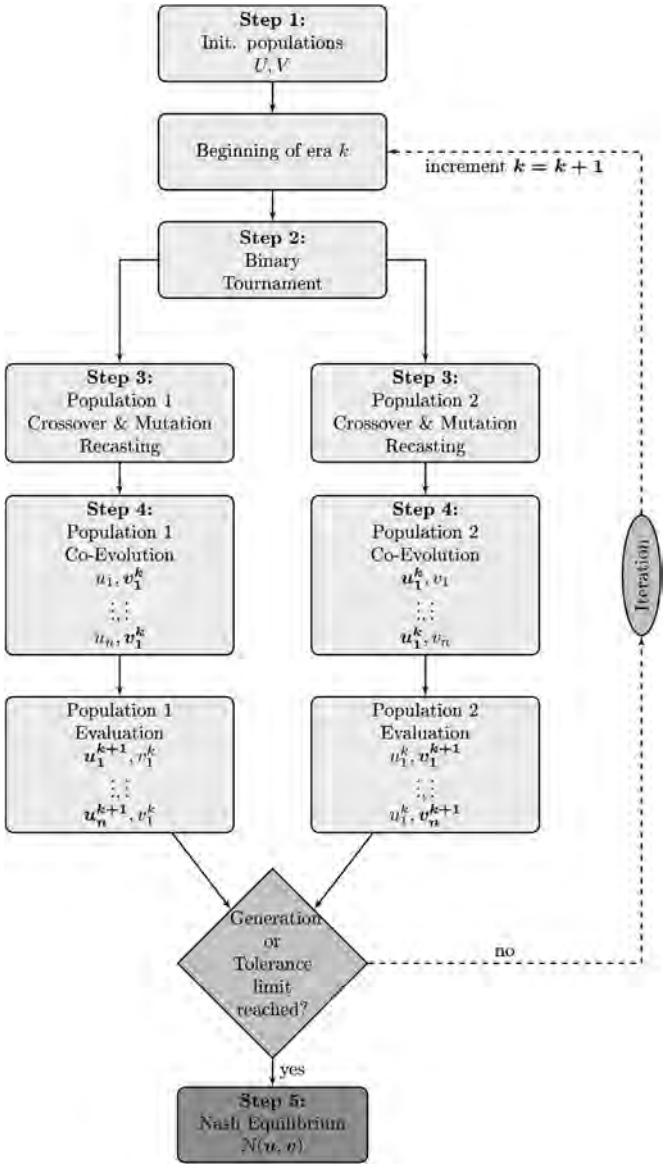


**Fig. 1.** Nash genetic algorithm structure.

And similarly, for player 2:

$$\begin{cases} \text{if } f_2(u_i^k, v^{k-1}) > f_2(u^{k-1}, v_i^k), & \text{fitness}_2 = 1 \\ \text{if } f_2(u_i^k, v^{k-1}) < f_2(u^{k-1}, v_i^k), & \text{fitness}_2 = -1 \\ \text{if } f_2(u_i^k, v^{k-1}) = f_2(u^{k-1}, v_i^k), & \text{fitness}_2 = 0 \end{cases} \tag{3}$$

In this way a simple sorting criterion could be established. For equal fitness value individuals are sorted on objective function $f_1$ for population 1 (player 1) and on objective function $f_2$ for player 2.

3. A mating pool for parent chromosome is generated and common GA techniques as crossover and mutation are performed on each player population. A second sorting procedure is needed after this evolution process in order to classify the new population made of parents and children together.
4. At the end of $k$-th generation optimization procedure player 1 communicates his own best value $u^k$ to player 2 who will use it at generation $k+1$ to generate its entire chromosome with a unique value for its first part, i.e. the one depending on player 1, while on the second part comes from common GAs crossover and mutation procedure. Conversely, player 2 communicates its own best value $v^k$ to player 1 who will use it at generation $k+1$, generating a population with a unique value for the second part of chromosome, i.e. the one depending on player 2.
5. A Nash equilibrium is found when a terminal period limit is reached, after repeating steps 2–4. This kind of structure for the algorithm is similar to those used by other researchers [7], with a major emphasis on fitness function consistency [30].

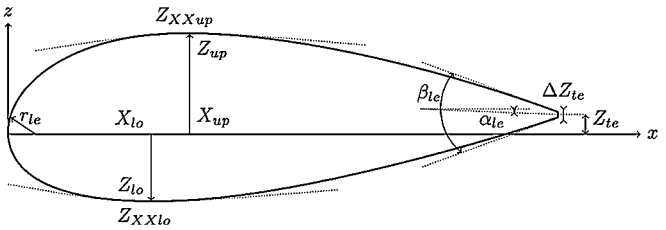


**Fig. 2.** PARSEC variable definition.

## 2. PARSEC and Games Theory

The idea to couple the PARSEC parameterization method [25,26] with Nash equilibrium solution give the chance to avoid a more arbitrary and less physically based airfoil geometry partition among the different objective functions (as shown in [8,29]), using instead a more engineering reliable variables assignment based on well-known airfoil shape parameter, as those present in literature [1].

The PARSEC airfoil shape parameterization [25,26] uses eleven parameters to represent an airfoil. In Fig. 2 is shown the PARSEC variables definition, which is then summarized in Table 1.

Parsec analytical formulation is shown in Eq. (4):

$$z_{up} = \sum_{i=1}^{n=6} a_{up}^i \cdot x^{i-\frac{1}{2}}, \qquad z_{lo} = \sum_{i=1}^{n=6} a_{lo}^i \cdot x^{i-\frac{1}{2}} \tag{4}$$

where $z_{up}$, $z_{lo}$ are, respectively, the vertical coordinate of the upper and lower surface, $x$ is the horizontal, or chord-wise, coordinate normalized in $[0, 1]$. The coefficients $a_{up}$, $a_{lo}$ have to be computed by using the 11 given parameters as follows:

$$C_{up} \times a_{up} = b_{up}, \qquad C_{lo} \times a_{lo} = b_{lo} \tag{5}$$

where both coefficient matrices ($C_{up}$, $C_{lo}$) and right hand sides ($b_{up}$, $b_{lo}$) are defined as shown in the matrices (6) and (7).

$$C_{up} = \begin{vmatrix} 1 & 1 & 1 & 1 & 1 & 1 \\ p_2^{\frac{1}{2}} & p_2^{\frac{3}{2}} & p_2^{\frac{5}{2}} & p_2^{\frac{7}{2}} & p_2^{\frac{9}{2}} & p_2^{\frac{11}{2}} \\ \frac{1}{2} & \frac{3}{2} & \frac{5}{2} & \frac{7}{2} & \frac{9}{2} & \frac{11}{2} \\ \frac{1}{2}p_2^{-\frac{1}{2}} & \frac{3}{2}p_2^{\frac{1}{2}} & \frac{5}{2}p_2^{\frac{3}{2}} & \frac{7}{2}p_2^{\frac{5}{2}} & \frac{9}{2}p_2^{\frac{7}{2}} & \frac{11}{2}p_2^{\frac{9}{2}} \\ -\frac{1}{4}p_2^{-\frac{3}{2}} & \frac{3}{4}p_2^{-\frac{1}{2}} & \frac{15}{4}p_2^{\frac{1}{2}} & \frac{15}{4}p_2^{\frac{1}{2}} & \frac{63}{4}p_2^{\frac{5}{2}} & \frac{99}{4}p_2^{\frac{7}{2}} \\ 1 & 0 & 0 & 0 & 0 & 0 \end{vmatrix} \tag{6}$$

$$b_{up} = \begin{vmatrix} p_8 + p_9/2 \\ p_3 \\ \tan(p_{10} - p_{11}/2) \\ 0 \\ \frac{p_4}{\sqrt{2p_1}} \end{vmatrix}, \qquad b_{lo} = \begin{vmatrix} p_8 - p_9/2 \\ p_6 \\ \tan(p_{10} + p_{11}/2) \\ 0 \\ \frac{p_4}{\sqrt{2p_1}} \end{vmatrix} \tag{7}$$

where coefficient matrix $C_{up}$ ($C_{lo}$) depends only on $p_2$ ($p_5$) (simply using $lo$ and 5 as subscript in Eq. (6)), while the right hand sides $b_{up}$, $b_{lo}$ differ for the use of $p_3$ instead of $p_6$ and parameters addiction/subtraction. The PARSEC method together with Games Theory equilibrium solution is used here to enhance the capability of common Pareto based optimization procedure. The idea is

**Table 1**
PARSEC parameters definition.

| PARSEC parameter | Geometry parameter | Definition |
|---|---|---|
| $p_1$ | $r_{le}$ | leading edge radius |
| $p_2$ | $X_{up}$ | upper crest position in horizontal coordinates |
| $p_3$ | $Z_{up}$ | upper crest position in vertical coordinates |
| $p_4$ | $Z_{XX_{up}}$ | upper crest curvature |
| $p_5$ | $X_{lo}$ | lower crest position in horizontal coordinates |
| $p_6$ | $Z_{lo}$ | lower crest position in vertical coordinates |
| $p_7$ | $Z_{XX_{lo}}$ | lower crest curvature |
| $p_8$ | $Z_{te}$ | trailing edge offset in vertical sense |
| $p_9$ | $\Delta Z_{te}$ | trailing edge thickness |
| $p_{10}$ | $\alpha_{te}$ | trailing edge direction |
| $p_{11}$ | $\beta_{te}$ | trailing edge wedge angle |

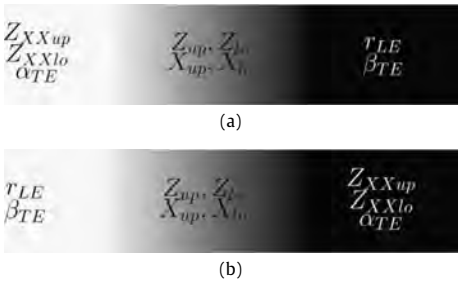


**Fig. 3.** (a) Variable assignment for $C_l$, (b) variable assignments for $C_d$.

to assign variables to player under a more physics related correspondence (as it can be seen in Fig. 3): the lift coefficient $C_l$ is mainly dependent on upper crest curvature ($Z_{XX_{up}}$ or shortened as $p_4$), the lower crest curvature ($Z_{XX_{lo}}$ or $p_7$), the trailing edge offset in vertical sense ($Z_{te}$ or $p_8$) and the trailing edge direction ($\alpha_{te}$ or $p_{10}$); the drag coefficient $C_d$ is mainly dependent on leading edge radius ($r_{le}$ or $p_1$), the trailing edge thickness ($\Delta Z_{te}$ or $p_9$) and trailing edge wedge angle ($\beta_{te}$ or $p_{11}$); both $C_l$ and $C_d$ are influenced by the upper crest position in horizontal and vertical coordinates ($X_{up}$ or $p_2$, $Z_{up}$ or $p_3$) and lower crest position in horizontal and vertical coordinates ($X_{lo}$ or $p_5$, $Z_{lo}$ or $p_6$). The choice of the portion of PARSEC variable subset that belongs to the Cl or Cd objective function (i.e. Cl or Cd player) is crucial to determine the capability of this combination in resulting closer (or farther) to (or from) Pareto front and to restrict the range of analyses. However it is not necessary to establish *a priori* the variables assignment to the players and, in theory, all the possible combinations should be considered (i.e. 55 combinations for this parameterization). Moreover the variables assignment is not linked to the objective function *a priori* but a more physical assignation could avoid the evaluation of the all possible combinations. For instance if the objective function is the $C_m$ instead $C_d$, the user can choose a different PARSEC variables assignment or consider all the possible combinations.

The white portion of Figs. 3(a) and 3(b) contains, respectively, the $C_l$ and $C_d$ related variables, that appears, of course, in the black portion of the other objective function. The gray area is used as a shared portion between players (i.e. objective functions for $C_l$ and $C_d$), and in the following a sensitivity analysis on gray variables distribution between players is conducted to evaluate Nash equilibrium with different strategy parameters set: the total number of combination is $C_{n=4,k=2} = \sum_{i \in n_0} \frac{n!}{i!(n-1)!} = 16$, where $n$ is the number of gray variables, $k$ the number of players among which the variables should be divided, and $n_0 = [0, \ldots, n]$. In Table 2 and Table 3 are summarized the variables' set assignments (see $x_1$, $x_2$ in Section 1) for all the combinations, identifying each variable with the PARSEC nomenclature. For both $C_l$ and $C_d$ variables' sets the top and bottom rows contain the black variable, while for both objective functions (or players as usually indicated in Games Theory) the gray variables are collected in the inner rows.

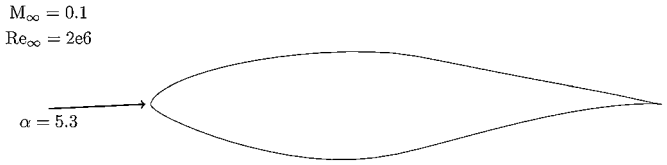


**Fig. 4.** Analysis condition starting from NREL S809 airfoil.

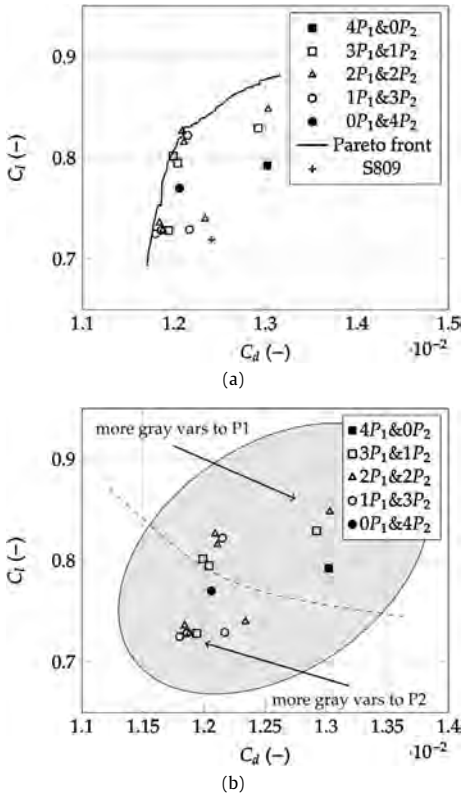


**Fig. 5.** (a) Nash GA set and Pareto front, (b) Nash equilibria set detail.

The variables' sets are collected in 5 groups in order to simplify the results discussion using: $4P_1\&0P_2$ for the case when all the gray variables belong to player 1, $3P_1\&1P_2$ for the case when 3 gray variables belong to player 1 and 1 to player 2, $2P_1\&2P_2$ for the case when all the gray variables are equally shared among the players, $1P_1\&3P_2$ for the case when 3 gray variables belong to player 2 and one to player 1, and finally $0P_1$ &$1P_2$ for the case when all the gray variables belong to player 2.

## 3. Results

It has been assumed that 2 of the eleven PARSEC variable, namely $Z_{te}$ and $\Delta Z_{te}$ are set equal to 0, it means closed trail-

**Table 2**
Nash GA set combinations 1–8.

| Case | 1 | 2 | 3 | 4 | 5 | 6 | 7 | 8 |
|---|---|---|---|---|---|---|---|---|
| | $p_4, p_7, p_8, p_{10}$ | | | | | | | |
| $C_l$ set | $p_2, p_3$ $p_5, p_6$ | $p_2, p_3$ $p_5$ | $p_2, p_3$ $p_6$ | $p_2, p_3$ | $p_2, p_5$ $p_6$ | $p_2, p_5$ | $p_2, p_6$ | $p_2$ |
| $C_d$ set | – | $p_6$ | $p_5$ | $p_5, p_6$ | $p_3$ | $p_3, p_6$ | $p_3, p_5$ | $p_3, p_5$ $p_6$ |
| | $p_1, p_9, p_{11}$ | | | | | | | |

**Table 3**
Nash GA set combinations 9–16.

| Case | 9 | 10 | 11 | 12 | 13 | 14 | 15 | 16 |
|---|---|---|---|---|---|---|---|---|
| | $p_4, p_7, p_8, p_{10}$ | | | | | | | |
| $C_l$ set | $p_3, p_5$ $p_6$ | $p_3, p_5$ | $p_3, p_6$ | $p_3$ | $p_5, p_6$ | $p_5$ | $p_6$ | – |
| $C_d$ set | $p_2$ | $p_2, p_6$ | $p_2, p_5$ | $p_2, p_5$ $p_6$ | $p_2, p_3$ | $p_2, p_3$ $p_6$ | $p_2, p_3$ $p_5$ | $p_2, p_3$ $p_5, p_6$ |
| | $p_1, p_9, p_{11}$ | | | | | | | |

ing edge (located at $(0, 1)$ coordinates), and the flow condition is a Reynolds number equal a to $\mathrm{Re}_\infty = 2\mathrm{E}6$, a Mach number equal to $M_\infty = 0.1$ and an angle of attack equal to $\alpha = 5.3^\circ$ with fixed transition location imposed at 5% in chord on upper and lower side, starting from an NREL S809 airfoil (see Fig. 4) using as external aerodynamic solver the open source panel method based code XFOIL [9].

### 3.1. Nash equilibrium

In this section the optimization results of the NREL S809 airfoil are shown. In particular, starting from the original airfoil coordinates, the optimization process has been run with a 10% of PARSEC parameters range of variation with respect to the starting ones, without any geometric or aerodynamic constraints. In order to attain an understanding of the implications in the Nash equilibrium point position introduced by the use of gray variables, each one of the 16 combinations described in Section 2 is considered. In Fig. 5 is exploited both the Nash equilibrium point position with respect to a normal genetic algorithm driven Pareto front as NSGA2 [6] (see Fig. 5(a)), and the internal relationship among the Nash equilibria set (see Fig. 5(b)).

In particular the filled square and circle indicates the assignment of all the gray variables, respectively, to players 1 and 2; the not filled squares and circles indicate, respectively an assignment of 3 gray variables to player 1 and 1 to player 2, and 1 gray variable to player 1 and 3 to player 2; the triangles indicate the assignment of 2 gray variables to both players.

The internal relationship among the points of the Nash *equilibria* set is emphasized in Fig. 5(b) where the gray ellipse contains all the points and the dashed curved line delimits two region: the upper one is the region of space variables where the Nash *equilibria* points are derived from an assignment of gray variables mostly to player 1, and *vice versa*. It is observed a clear division of Nash *equilibria* loci in a subset dominated from player 1 requirement, i.e. the highest possible $C_l$ value, indicated by a not-filled-squares majority located in the upper-right portion of the gray ellipse, and a subset dominated from player 2 requirement, i.e. the lowest possible $C_d$ value, indicated by a not-filled-circles majority located in the lower-left portion of the gray ellipse. The dotted curved line is a simple sketch of the division between these two regions, where also most of the triangles are located, corresponding to an even partition of gray variables among the players.

In particular, the Nash equilibria points for equally shared gray variables that belong to the upper region of Fig. 5(b) are the one indicated in Table 2 and Table 3 as cases 6, 10 and 13, while the one that belong to the lower region are the cases indicated with 4, 7 and 11. The Nash equilibria points for gray variables mostly belonging to $C_l$ player (boxes) and $C_d$ (circles) player are located, respectively, in the upper and lower region emphasized in Fig. 5(b). The relationship between the Nash equilibria set and the Pareto front is exploited in Fig. 5(a).

The Nash equilibria points for gray variables assigned completely to players 1 and 2 (respectively filled square and circle) are almost as close to Pareto front as the average of the other distributions, with the $C_d$ dominated Nash equilibrium point being the closest among the two. The other distributions of gray variables show at least one point very close to Pareto front. The Nash equilibria points that are located closer the Pareto front are 5 (they are more evident in Fig. 6): two of them belong to the set $3\mathrm{P}_1\&1\mathrm{P}_2$ cases 5 and 9 from Table 2 and Table 3, two of them to the set $2\mathrm{P}_1\&2\mathrm{P}_2$ cases 6 and 13 from Table 2 and Table 3, and one to the set $1\mathrm{P}_1\&3\mathrm{P}_2$ case 14 from Table 3. In Fig. 7 there are shown both the shape (7(a)) and the pressure coefficient, $C_P$, distribution chord-wise (7(b)). In black is indicated the solution for a Nash equilibrium in which player 1 holds all the gray variables, for which the lift coefficient, $C_l$, requirement is pursued by the majority of the chromosome, so that the final shape exhibits higher thickness, longer suction portion and bigger trailing edge curvature. In gray is indicated the solution for a Nash equilibrium in which player 2 holds all the gray variables, for which the drag coefficient, $C_d$, requirement is pursued by the majority of the chromosome, so that the final shape exhibits lower thickness and a sharper nose portion.

It is interesting to show some optimized airfoil geometries and their pressure coefficient distributions which belong to the Pareto front. In particular four distinct airfoils have been chosen, located in such manner to cover the entire front, as shown in Fig. 8. These geometries are compared to the original S809 airfoil in Fig. 9 and pressure coefficients in Fig. 10. Once again the airfoil with the lower drag coefficient (named Pareto1) has a lower thickness and a sharper nose especially in the lower surface. Pareto1 airfoil is very close to the airfoil named 0P1&4P2 both in terms geometry and pressure distribution (see Fig. 7(b) and Fig. 10). This means that both methodologies (Nash GA and GA) follow the same direction during the optimization processes. Considering other airfoils (Pareto2, Pareto3 and Pareto4) the effect during the optimization is to increase the airfoil thickness and camber, especially at the trailing edge, to increase lift coefficient. Once again both geometry

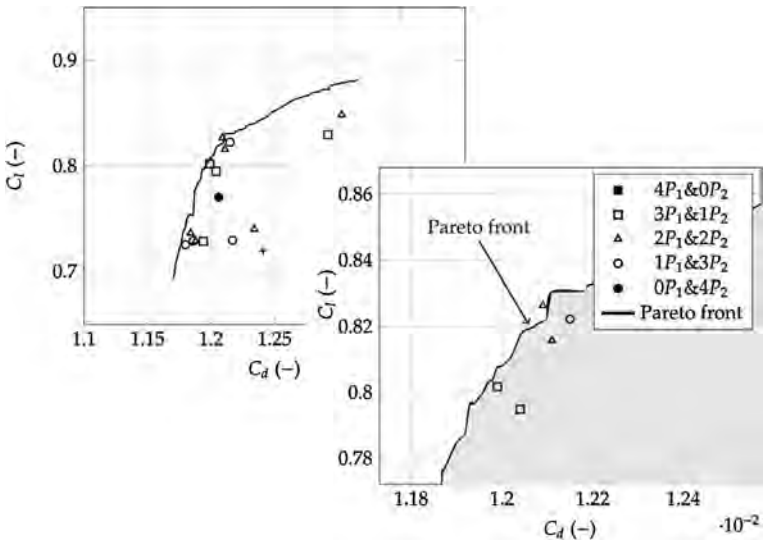


**Fig. 6.** Nash GA set and Pareto front in detail.

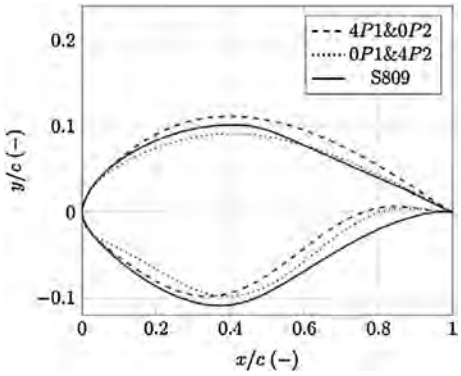


(a)

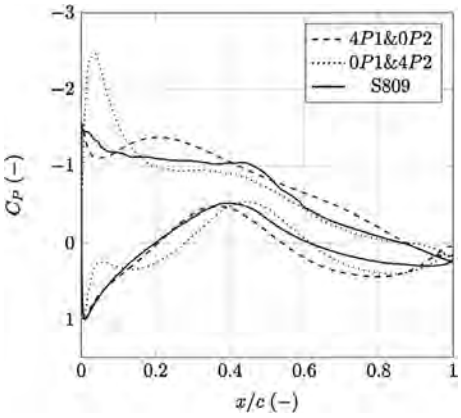


(b)

**Fig. 7.** (a) Nash optimized airfoil shapes, (b) Nash optimized pressure coefficient distribution.

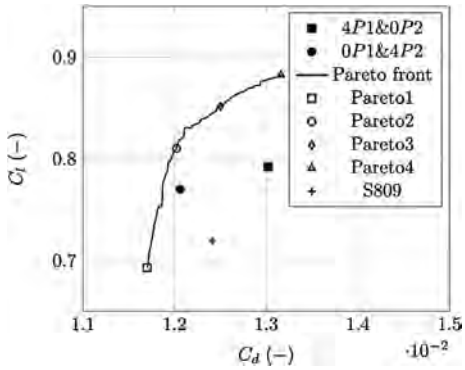


**Fig. 8.** Optimized airfoil positions on the Pareto frontier.

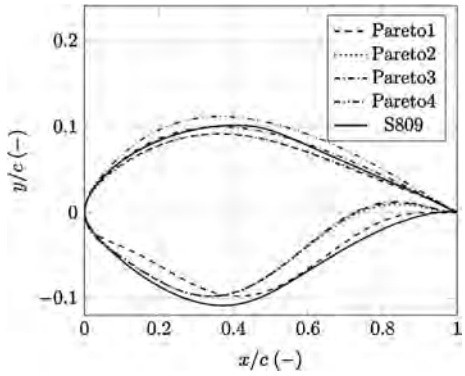


**Fig. 9.** Pareto optimized airfoil shapes.

and pressure coefficient of airfoil Pareto4 (which has the higher lift coefficient) are similar to the airfoil named 4P1&0P2.

### 3.2. Nash equilibrium for constrained thickness

In this section the constrained optimization results of the NREL S809 airfoil are shown. Airfoil thickness has been constrained at 20% of the chord in order to understand how the Nash equilibrium set would behave when some limitations in airfoil geometry are introduced, as could be observed when other issues other than aerodynamic are pursuit: e.g. section inertia for structural stiffness requirement and section volume for the needs of other devices and components to be located.

As for the unconstrained optimization case, the distribution of Nash equilibrium points reflects what already has been said for the results shown in Fig. 5: the point with four gray variables belonging to $C_l$ ($C_d$) is located toward a higher $C_l$ (lower $C_d$) region with respect to the mean distribution, and the same holds for the points with only three gray variables belonging to $C_l$ ($C_d$), as shown in Fig. 11. Again the Nash equilibrium points with equally shared

**Table 4**
Pareto and Nash equilibrium time to compute.

| Case | Pop. size | Gen. limit | Time to compute (s)[1] | Time to compute one Nash point (s)[1] | Convergence error[2] |
|---|---|---|---|---|---|
| Nash | 20 | 20 | 491 469 | 30 717 | ∼5% |
| | 30 | 20 | 698 535 | 43 658 | ∼3% |
| | 40 | 20 | 938 562 | 58 660 | ∼0.2% |
| | 100 | 40 | 4 567 652 | 285 478 | ∼0.002% |
| Pareto | 20 | 20 | 103 584 | | See Fig. 13 |
| | 30 | 20 | 158 945 | | See Fig. 13 |
| | 40 | 20 | 210 701 | | See Fig. 13 |
| | 100 | 100 | 2 512 491 | | See Fig. 13 |

[1] On an Intel core 2 duo CPU @1.8Ghz, without using parallel computing.
[2] On 10 iterations.

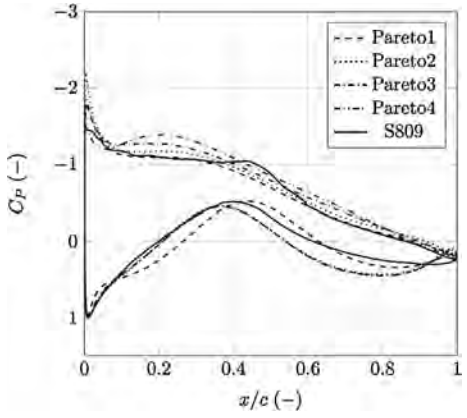


**Fig. 10.** Pareto optimized pressure coefficient distribution.

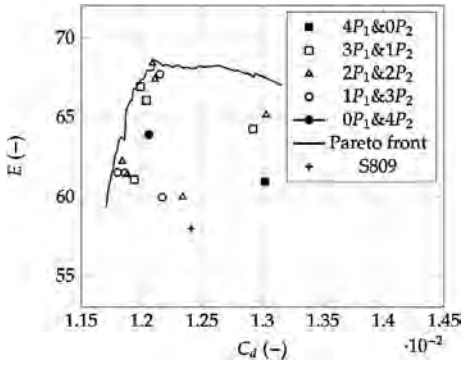


(a)

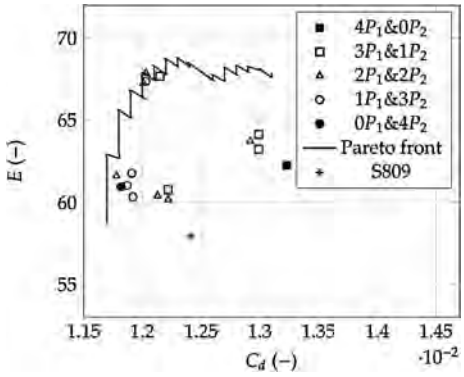


(b)

**Fig. 11.** Results for constrained optimization.

gray variables among $C_l$ and $C_d$ objective functions are spread almost uniformly within the whole region and are the closest to the Pareto Front (see Fig. 11). The S809 airfoil is intended to be used in wind turbine application mostly because of its aerodynamic efficiency $E = C_l/C_d$ together with its inertia characteristics necessary to withstand aerodynamic load at the blade innermost region (i.e. root). The optimizations performed here are intrinsically conservative because of the imposed transition from laminar to turbulent flow at 5% chord, so that the efficiency would be far lower than the one available in clean configuration: this is closer to the situation of a wind turbine blade operating a long time after the maintenance and cleaning service of the leading edge, i.e. the case responsible of the worse power extraction performance. In order to show that the solutions derived from both Pareto front and Nash equilibria set are able to increase the performance of such a wind energy dedicated airfoil, in Fig. 12 is shown aerodynamic efficiency distribution with respect to the drag coefficient for both unconstrained and constrained optimization case.

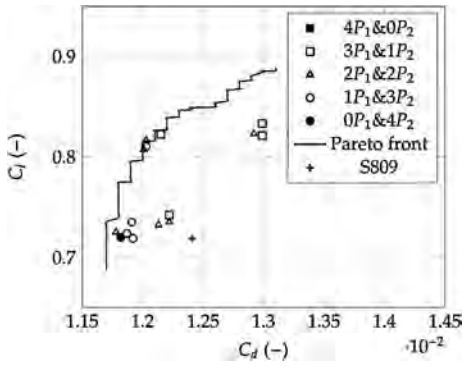


**Fig. 12.** (a) Aerodynamic efficiency vs. drag coefficient, not constrained case, (b) aerodynamic efficiency vs. drag coefficient, constrained case $\tau = 20\%$.

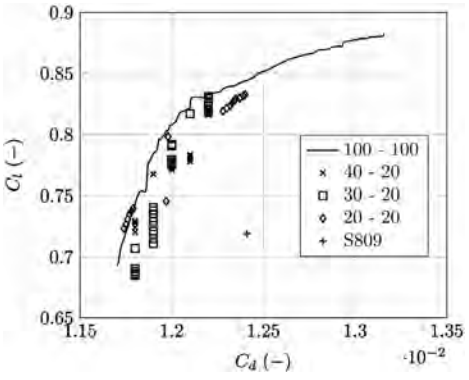


**Fig. 13.** Pareto frontier convergence.

### 3.3. Computational time comparison

Finally, some additional information on the computational time needed for both Pareto and Nash equilibrium calculations could be given as in Table 4. It is clearly attained an almost perfect linear re-

lation between population size (or generation limit) and total time, while keeping the generation limit (or population size) constant. The strong difference between these results are the population size and the generation limit needed: in a Pareto optimization, a large population is needed to sample accurately all the front, but the evolution of a so large population is slow, making necessary a long generation limit. A Game Theory-based optimization model can be useful to find rapidly a unique solution that averages the overall Pareto results. In the performed tests more than one Nash solutions are near-Pareto, using a genetic algorithm based on small populations. This means in a reduced amount of configuration analysis and consequently a decreased computational time. In the same time (or no. of iterations), the Pareto based optimization algorithm has not computed a stable front (see Fig. 13), so the result cannot be guaranteed. The Nash based algorithm needs less iterations (see Table 4) to get the final result (the Nash equilibrium point).

## 4. Conclusions

In this work an optimization technique that deals with PARSEC parameterization method and Nash equilibrium genetic algorithm is presented. It has been shown that the Nash equilibrium points lie on the Pareto front, but with respect to the Pareto front solutions they have been obtained in very less time, so that a Pareto front could be maybe computed starting from some of them, so achieving more rapidly the convergence criteria. When one of the two objective functions should be considered more important than the other, without using some weight method one could substitute the Nash equilibrium optimization algorithm with a Stackelberg strategy optimization algorithm. The risk of finding only one among multiple Nash equilibria points could be reduced using a multi-modal approach. Some operating condition that should be considered as off-design could not be addressed with a panel method as XFOIL, so that a more time consuming fluid dynamic solver, as StarCCM+ or OpenFOAM, should be taken into account.

Finally, the extension of this optimization methodology to a 3D case as a wing or blade would be treated in the next future again starting from the PARSEC parameterization for three-dimensional shapes.

## References


[1] I.H. Abbott, A.E. von Doenhoff, Theory of Wing Sections: Including a Summary of Airfoil Data, Dover Publications, ISBN 978-0486605869, 1959.

[2] T. Basar, G.J. Olsder, Dynamic Noncooperative Game Theory, Classics in Applied Mathematics, vol. 23, Society for Industrial and Applied Mathematics (SIAM), Philadelphia, PA, 1995.

[3] P. Castonguay, S. Nadarajah, Effect of shape parameterization on aerodynamic shape optimization, in: 45th AIAA Aerospace Science Meeting and Exhibit, Reno, Nevada, 8–11 January 2007.

[4] E. D'Amato, E. Daniele, L. Mallozzi, G. Petrone, Equilibrium strategies via GA to Stackelberg games under multiple follower's best reply, Int. J. Intell. Syst. 27 (2012), http://dx.doi.org/10.1002/int.21514.

[5] E. D'Amato, E. Daniele, L. Mallozzi, G. Petrone, S. Tancredi, A hierarchical multimodal hybrid Stackelberg–Nash GA for a leader with multiple followers game, in: A. Sorokin, R. Murphey, M.T. Thai, P.M. Pardalos (Eds.), Dynamics of Information Systems: Mathematical Foundations, in: Springer Proceedings in Mathematics & Statistics, vol. 20, Springer-Verlag, USA, ISBN 9781461439059, 2012, pp. 267–280.

[6] K. Deb, Multi-Objective Optimization Using Evolutionary Algorithms, Wiley, USA, ISBN 978-0471873396, 2001.

[7] K. Deb, S. Agrawal, A. Pratap, T. Meyarivan, A fast elitist non-dominated sorting genetic algorithm for multi-objective optimization: NSGA-II, in: Marc Schoenauer, K. Deb, G. Rudolph, Xin Yao, Evelyne Lutton, Juan Julian Merelo, Hans-Paul Schwefel (Eds.), Parallel Problem Solving from Nature – PPSN VI, Springer, Berlin, 2000, pp. 849–858.

[8] R.W. Derksen, T. Rogalsky, Bezier-PARSEC: An optimized aerofoil parameterization for design, Adv. Eng. Softw. 41 (2010) 923–930.

[9] M. Drela, XFOIL: An analyse and design system for low Reynolds number airfoils, in: Low Reynolds Number Aerodynamics, in: Lecture Notes in Engineering, vol. 54, Springer-Verlag, 1989.

[10] D. Fudenberg, J. Tirole, Game Theory, MIT Press, Boston, USA, ISBN 978-0262061414, 1991.

[11] F. Grasso, Multi-objective numerical optimization applied to aircraft design, PhD thesis, Aerospace Engineering, Department of Aerospace Engineering, University of Naples Federico II, 2008.

[12] R.L. Haupt, S.E. Haupt, Practical Genetic Algorithms, Wiley–Interscience, ISBN 978-0471455653, 2004.

[13] R.M. Hicks, P.A. Henne, Wing design by numerical optimization, J. Aircr. 15 (7) (1978) 407–412.

[14] R.M. Hicks, G.N. Vanderplaats, Application of numerical optimization to the design of low-speed airfoils, NASA TM X-3213, Ames Research Center, Moffet Field, CA, 1975.

[15] M. Khurana, Airfoil geometry parameterization through shape optimizer and computational fluid dynamics, in: 46th AIAA Aerospace Sciences Meeting and Exhibit, 7th–10th January 2008, Grand Sierra Resort, Reno, Nevada.

[16] E. Makoto, Wind turbine airfoil optimization by particle swarm method, Ms.D. thesis, Department of Mechanical and Aerospace Engineering, Case Western Reserve University, 2011.

[17] L. Mallozzi, E. D'Amato, E. Daniele, G. Petrone, *N* leader–*M* follower coalition games with genetic algorithms and applications, in: C. Poloni, D. Quagliarella, J. Priaux, N. Gauger, K. Giannakoglou (Eds.), Proceedings of EUROGEN2011 Evolutionary and Deterministic Methods for Design, Optimization and Control, ISBN 9788890632303, 2011, pp. 852–866.

[18] L. Mallozzi, E. D'Amato, E. Daniele, G. Petrone, Waiting time costs in a bilevel location–allocation problem, in: L.A. Petrosyan, N.A. Zenkevich (Eds.), Contributions to Game Theory and Management V, Graduate School of Management, St. Petersburg University, Russia, 2012, pp. 178–186.

[19] J.F. Nash Jr., Non-cooperative games, Ann. Math. (2) 54 (2) (1951) 286–295, http://www.jstor.org/stable/1969529.

[20] M.Y.V. Pehlivanoglu, Representation method effects on vibrational genetic algorithm in 2-D airfoil design, J. Aeronaut. Space Technol. 4 (2) (July 2009) 7–13.

[21] J. Pèriaux, D.S. Lee, L.F. Gonzalez, K. Srinivas, Fast reconstruction of aerodynamic shapes using evolutionary algorithms and virtual Nash strategies in a CFD design environment, J. Comput. Appl. Math. 232 (2009) 61–71.

[22] Q. Ruizhan, Z. Ziqiang, A variable fidelity optimization framework using second-order multi-point additive scaling functions applied to airfoil design, in: 25th International Congress of the Aeronautical Sciences, 3–8 September 2006.

[23] J.A. Samareh, A survey of shape parameterization techniques, in: CEAS/AIAA/ICASE/NASA Langley International Forum on Aeroelasticity and Structural Dynamics, Williamsburg, VA, June 22–25, 1999.

[24] A. Shahrokhi, A. Jahangirian, The effects of shape parametrization on the efficiency of evolutionary design optimization for viscous transonic airfoils, J. Aerosp. Sci. Technol. 5 (1) (2008) 35–43.

[25] H. Sobieczky, Geometry generator for CFD and applied aerodynamics, in: Courses and Lecture International, 1997.

[26] H. Sobieczky, Parametric airfoils and wings, in: K. Fujii, G.S. Dulikravich (Eds.), Notes on Numerical Fluid Mechanics, vol. 68, Vieweg Verlag, 1998, pp. 71–88.

[27] W. Song, A.J. Keane, A study of shape parameterisation methods for airfoil optimisation, AIAA 2004-4482, in: 10th AIAA/ISSMO Multidisciplinary Analysis and Optimization Conference, Albany, New York, 30 August–4 September, 2004.

[28] S. Tancredi, E. D'Amato, E. Daniele, P. Della Vecchia, G. Petrone, A Nash equilibrium-genetic algorithm optimization code for structural problems. Test case: an aluminum plate subjected to low velocity impact events, in: 2010 ENGINSOFT International Conference, CAE Technologies for Industry and ANSYS Italian Conference Proceedings, 21–22 October, Brescia, Italy, 2010.

[29] Z. Tang, J.A. Désidéri, J. Periaux, Multicriterion aerodynamic shape design optimization and inverse problems using control theory and nash games, J. Optim. Theory Appl. 135 (2007) 599–622.

[30] J.F. Wang, J. Periaux, M. Sefrioui, Parallel evolutionary algorithms for optimization problems in aerospace engineering, J. Comput. Appl. Math. 149 (2002) 155–169.

[31] H.Y. Wu, S. Yang, F. Liu, Comparison of three geometric representations of airfoils for aerodynamic optimization, in: 16th AIAA Computational Fluid Dynamics Conference, Orlando, FL, 23–26 June 2003.